CHINA FOUNDRY Research & Development
Vol. 18 No. 3 May 2021
https://doi.org/10.1007/s41230-021-9020-6

TiN/γ-Fe interface orientation relationship and formation mechanism of TiN precipitates in Mn18Cr2 steel

Zheng-hui Wang[1,3], *Jing-pei Xie[2,4], **Qian Li[1,3], Wen-yan Wang[2,4], Ai-qin Wang[2,4], Pei Liu[2,4]

1. School of Materials Science and Engineering, Zhengzhou University, Zhengzhou 450001, China

2. School of Materials Science and Engineering, Henan University of Science and Technology, Luoyang 471023, China

3. National Center of International Research for Micro-nano Molding Technology, Zhengzhou University, Zhengzhou 450001, China

4. Provincial and Ministerial Co-construction of Collaborative Innovation Center for Non-ferrous Metal New Materials and Advanced Processing Technology, Henan University of Science and Technology, Luoyang 471023, China

Abstract: A Mn18Cr2 steel containing TiN precipitates was fabricated by vacuum induction melting. The morphology of TiN precipitates and the interface orientation relationship between TiN and γ-Fe were characterized by means of SEM, TEM and SAED, and the formation mechanism of TiN precipitates in Mn18Cr2 steel was clarified. Results show that the TiN precipitates are more likely to exhibit a cubic-shaped morphology and form both within the grain and at the grain boundary of γ-Fe. The interface orientation relationship between TiN and γ-Fe is determined as follows: $(100)_{TiN}//(1\bar{1}1)_{\gamma\text{-}Fe}$, $[0\bar{1}1]_{TiN}//[\bar{1}12]_{\gamma\text{-}Fe}$. Because of the smallest interfacial misfit, the secondary close-packed lane {100} of TiN preferentially combines with the close-packed plane {111} of γ-Fe during the precipitation in order to minimize the interface energy. After nucleation, the TiN precipitates exhibit cubic appearance due to the fact that the TiN has a FCC structure with rock salt type structure. This study provides reference for the material design of the austenitic high-manganese steels with excellent yield strength.

Key words: Mn18Cr2 steel; TiN precipitates; interface orientation relationship; interface misfit

CLC numbers: TG142.11 **Document code:** A **Article ID:** 1672-6421(2021)03-180-05

1 Introduction

Austenitic high-manganese steel (≥15wt.% Mn) has a good combination of high strength and high ductility due to its capability of obtaining single austenitic structure through solid solution. Therefore, the austenitic high-manganese steel has attracted much attention in many structural applications exposed to heavy loads, such as the shovel tooth of an excavator, the rolling mortar wall of a cone crusher and the lining plate of a ball mill [1-6]. However, the application of austenitic high-manganese steels is limited due to their low yield strength compared to other structural materials. Therefore, many investigations have been performed to improve the yield strength of austenitic high-manganese steels by the method of micro-alloying, adding RE modifier or ceramic particles via the strengthening mechanisms of solid solution strengthening, precipitation strengthening, and grain refinement [7-12].

Among the various strengthening methods, the dispersive precipitation of the ceramic particle TiN in austenitic high-manganese steels has attracted much attention [13-14], because the fine ceramic particle TiN could not only hinder the dislocation propagation, but can also act as the heterogeneous site and refine the solidified microstructure, which is beneficial for improving the yield strength of the austenitic high-manganese steels. However, few studies can be found focusing on the morphology, interface orientation relationships and formation mechanisms of TiN precipitates in austenitic high-manganese steels, which prevents the microstructure control and performance optimization of austenitic high-manganese steels containing TiN precipitates.

***Jing-pei Xie**

Ph. D., Professor. His main research interest is mainly focused on metal matrix composites. He has completed 45 national and provincial scientific research projects, which were financially supported by the National Natural Science Foundation of China, and the National Science and Technology Support Program. He has received one Second Prize and one Third Prize for Progress in Science and Technology of China. To date, he has published 8 books and more than 400 academic papers, and holds 48 invention patents of China.

E-mail: xiejp@haust.edu.cn

****Qian Li**

E-mail: qianli@zzu.edu.cn

Received: 2020-12-08; Accepted: 2021-02-03

In the present study, a Mn18Cr2 steel containing TiN precipitates was fabricated. The morphology of TiN precipitates and the TiN/austenite interface orientation relationship were characterized by means of SEM, TEM and SAED, and the formation mechanism of TiN precipitates in Mn18Cr2 steel was also investigated.

2 Experimental method

Table 1 shows the nominal chemical composition of the experimental alloy in the present work. The Mn18Cr2 steel was firstly melted in a vacuum induction furnace at 1,883 K for about 30 min, and then poured into magnesia sand molds with the dimensions of 150 mm height and 70 mm inner diameter. Then, the cast ingot was heated at 1,353 K for 2 h and water quenched for austenizing.

SEM samples with the dimensions of 10 mm × 10 mm × 10 mm and TEM samples with the dimensions of 10 mm × 10 mm × 0.3 mm were cut from the Mn18Cr2 steel blocks. The SEM samples were first ground successively with 400, 800, 1000 and 2000 grade SiC papers and then carefully polished with 2.5, 1.5 and 0.5 μm polishing pastes. The SEM observations were performed on the JSM-5610LV scanning electron microscopy. The TEM samples were mechanically polished to 50–60 μm thick, and then were ion milled by Gatan-691 to obtain a large thin area. Then, the TEM investigations were carried out on the JEM-2100 transmission electron microscope.

Table 1: Chemical compositions of Mn18Cr2 steel (wt.%)

C	Mn	Cr	Ti	N	S	P	Fe
1.30	18.20	2.10	0.25	0.25	0.056	0.040	Bal.

3 Results and discussion

3.1 Morphology of TiN precipitates

Figure 1 shows the SEM morphology of TiN precipitates. It can be seen that the TiN precipitates form both within the grain and at the grain boundary of γ-Fe, and exhibit a cubic-shaped morphology. As a general rule, the close-packed plane {111} of FCC crystal has the lowest energy, and thus the morphology of FCC crystal during the solidification should be octahedral. However, the TiN precipitates in the present work exhibit cubic morphology, which indicates that the surfaces of TiN precipitates are more likely to be the secondary close-packed lane {100}. Therefore, it can be inferred that there must be some other factors, such as the lattice misfit or the interface energy between the TiN precipitate and γ-Fe, affect the growth behavior and change the final morphology of TiN precipitates.

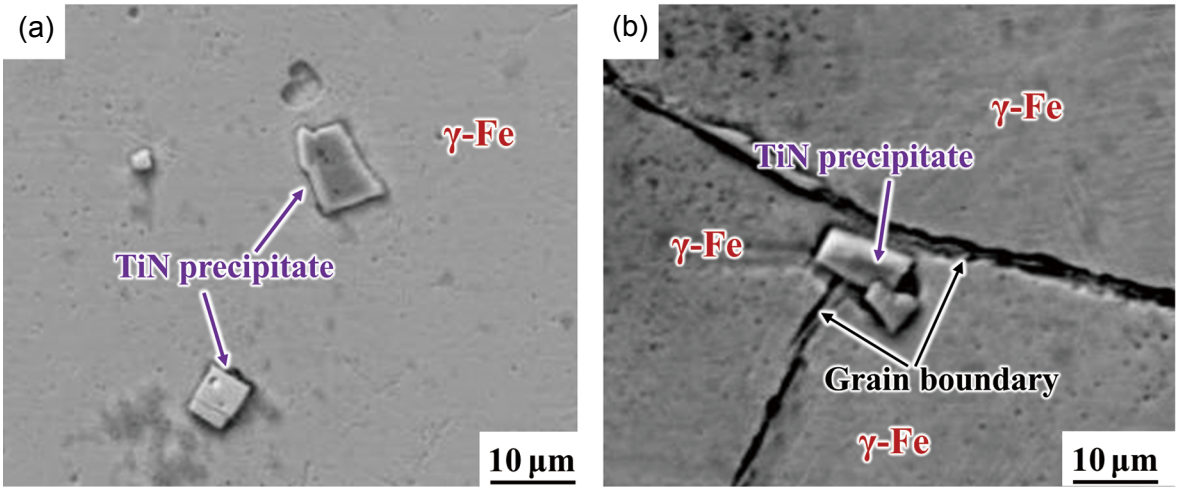

Fig. 1: SEM morphology of TiN precipitate distributed within the grain (a) and at grain boundary (b) of γ-Fe

3.2 Crystal orientation relationship between TiN and γ-Fe

Figure 2(a) shows a typical TEM image of the TiN/γ-Fe interface. It can be seen that the interface between TiN and γ-Fe is clean and flat. Figure 2(b) shows the SAED pattern from the TiN/γ-Fe interface. As shown in Fig. 2(b), the incident beam is parallel to $[0\bar{1}1]_{TiN}$ and $[\bar{1}12]_{\gamma\text{-Fe}}$, and the (200) plane of TiN is parallel to the $(1\bar{1}1)$ plane of γ-Fe. Thus, the crystal orientation relationship between TiN and γ-Fe is determined as follows:

$$(100)_{TiN}//(1\bar{1}1)_{\gamma\text{-Fe}},\ [0\bar{1}1]_{TiN}//[\bar{1}12]_{\gamma\text{-Fe}}$$

In order to depict the high symmetry elements along the $[0\bar{1}1]_{TiN}$ $//[\bar{1}12]_{\gamma\text{-Fe}}$, as shown in Fig. 2(c), stereographic projections of plane indexes of TiN and γ-Fe along the $[0\bar{1}1]_{TiN}//[\bar{1}12]_{\gamma\text{-Fe}}$ were superimposed according to the above crystal orientation relationship. Except for the above mentioned $(100)_{TiN}//(1\bar{1}1)_{\gamma\text{-Fe}}$,

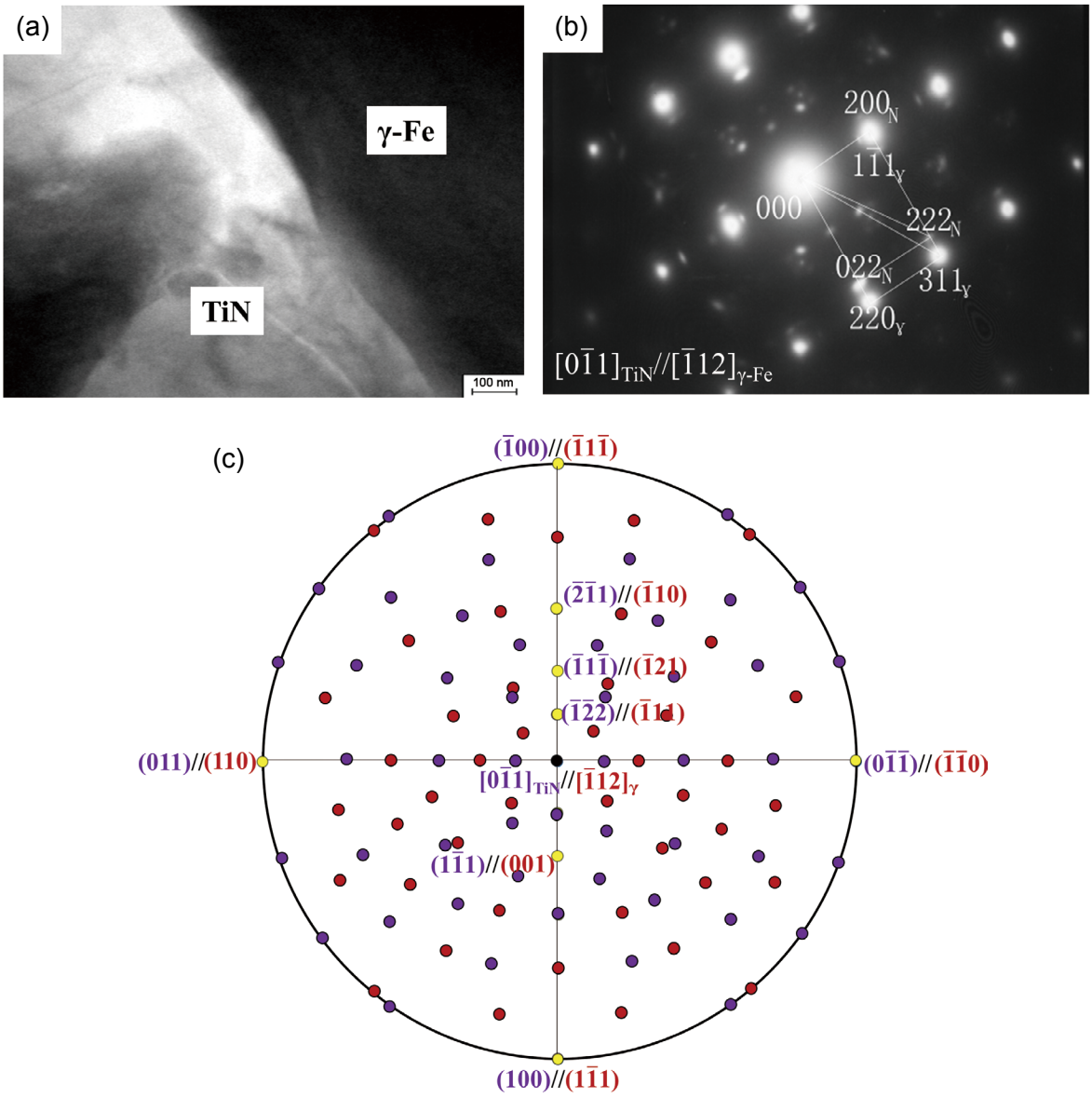

Fig. 2: TEM morphology of TiN/γ-Fe interface (a); SEAD from TiN/γ-Fe interface (b); stereographic projection showing orientation relationship along $[0\bar{1}1]_{TiN}//[\bar{1}12]_{\gamma\text{-Fe}}$ (c)

the following crystal orientation relationships also exist:

$$(011)_{TiN} // (110)_{\gamma\text{-Fe}}$$

$$(\bar{2}\bar{1}1)_{TiN} // (\bar{1}10)_{\gamma\text{-Fe}}$$

$$(\bar{1}1\bar{1})_{TiN} // (\bar{1}21)_{\gamma\text{-Fe}}$$

3.3 Growth mechanisms of TiN precipitates

It is well known that when a new phase tends to precipitate from the matrix, it preferentially nucleates at the close-packed planes of the matrix in order to minimize the interface energy between the precipitate and matrix. In this case, the lattice misfit along the precipitate/matrix interface has a decisive effect on the precipitate nucleation and growth behavior, because the driving force for the nucleation and growth of an precipitate increases monotonically with the increase of the lattice misfit between the matrix and the precipitate [15]. Thus, the interfacial misfit between the close-packed plane (111) of γ-Fe and three TiN surfaces, i.e., TiN(111), TiN(100) and TiN(110), was calculated. Figure 3 shows the crystal and surface atomic structures for the γ-Fe and TiN, and the summary of the calculated interfacial misfit between γ-Fe and TiN is shown in Table 2. It could be clearly seen from Table 2 that when the interfacial orientation relationship is γ-Fe($1\bar{1}1$)// TiN(100) and γ-Fe[$\bar{1}12$]//TiN[$0\bar{1}1$], the interfacial misfit is the smallest. This indicated that the secondary close-packed lane {100} of TiN has the best matching relationship with the close-packed plane {111} of γ-Fe, and thus the secondary close-packed plane {100} of TiN would preferentially combine with the close-packed plane {111} of γ-Fe during the precipitation in order to minimize the interface energy. The TiN precipitates exhibit cubic appearance due to the fact that the TiN has a FCC structure with rock salt type structure.

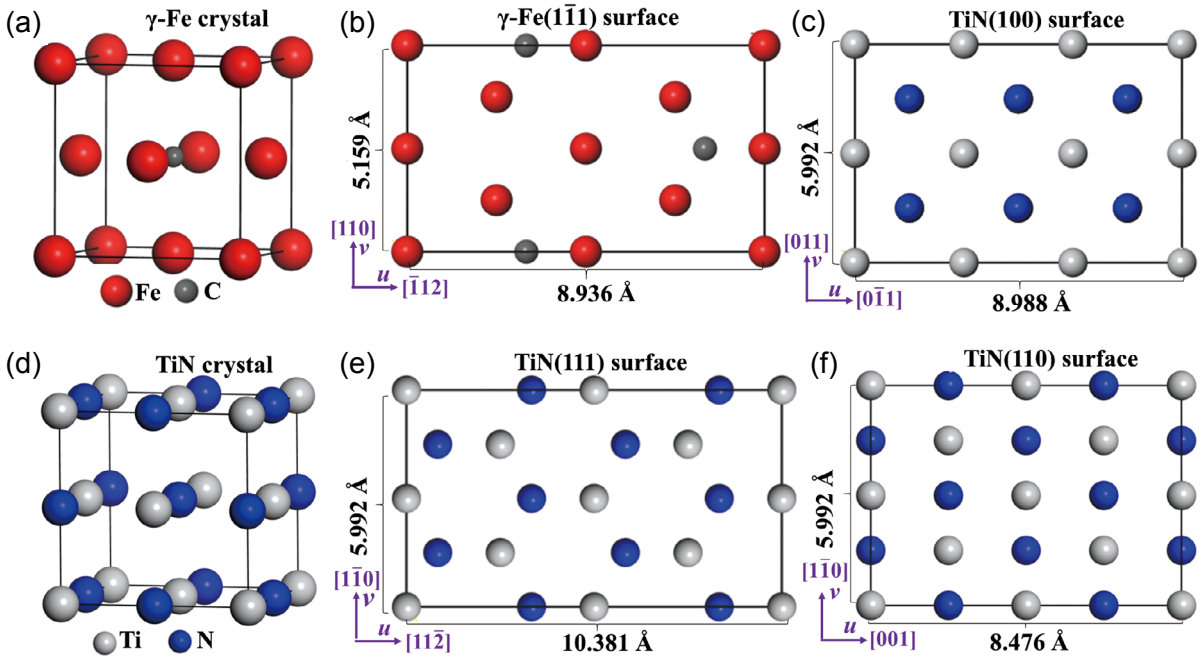

Fig. 3: Crystal and surface atomic structures of γ-Fe (a–b) and TiN (c–f)

Table 2: Calculated interfacial misfit between γ-Fe and TiN

Number	Orientation relationship	Interfacial misfit
1	γ-Fe(1$\bar{1}$1)//TiN(111) γ-Fe[110]//TiN[1$\bar{1}$0] in *v* direction γ-Fe[$\bar{1}$12]//TiN[11$\bar{2}$] in *u* direction	13.9% in *v* direction 13.9% in *u* direction
2	γ-Fe(1$\bar{1}$1)//TiN(100) γ-Fe[110]//TiN[011] in *v* direction γ-Fe[$\bar{1}$12]//TiN[0$\bar{1}$1] in *u* direction	13.9% in *v* direction 0.58% in *u* direction
3	γ-Fe(1$\bar{1}$1)//TiN(110) γ-Fe[110]//TiN[1$\bar{1}$0] in *v* direction γ-Fe[$\bar{1}$12]//TiN[001] in *u* direction	13.9% in *v* direction 5.42% in *u* direction

4 Conclusions

In this work, a Mn18Cr2 steel containing TiN precipitates was fabricated by vacuum induction melting. The morphology of TiN precipitates, TiN/γ-Fe interface orientation relationship and the formation mechanism of TiN precipitates were investigated. The following conclusions can be obtained:

(1) The TiN precipitates can form both within the grain and at the grain boundary of γ-Fe, and the TiN precipitates exhibit a cubic-shaped morphology.

(2) The interface orientation relationship between TiN and γ-Fe can be determined as follows: $(100)_{TiN}$ // $(1\bar{1}1)_{\gamma\text{-Fe}}$, $[0\bar{1}1]_{TiN}$ // $[\bar{1}12]_{\gamma\text{-Fe}}$.

(3) Because of the smallest interfacial misfit, the secondary close-packed plane {100} of TiN preferentially combines with the close-packed plane {111} of γ-Fe during the precipitation in order to minimize the interface energy. The TiN precipitates exhibit cubic appearance due to the fact that the TiN has a FCC structure with rock salt type structure.

Acknowledgements

The authors acknowledge the financial support from the National Natural Science Foundation of China (Grant No. U1604251) and the Major Scientific and Technological Project of Luoyang, China (Grant No. 2001017A).

References

[1] Sohn S S, Hong S, Lee J, et al. Effects of Mn and Al contents on cryogenic-temperature tensile and Charpy impact properties in four austenitic high-Mn steels. Acta Mater., 2015, 100: 39–52.

[2] Wang Z, Lin T, He X B, et al. Microstructure and properties of TiC-high manganese steel cermet prepared by different sintering processes. J. Alloys Compd., 2015, 650: 918–924.
[3] Lee S I, Lee S Y, Han J, et al. Deformation behavior and tensile properties of an austenitic Fe-24Mn-4Cr-0.5C high-manganese steel: Effect of grain size. Mater. Sci. Eng. A, 2019, 742: 334–343.
[4] Bambach M, Conrads L, Daamen M, et al. Enhancing the crashworthiness of high-manganese steel by strain-hardening engineering, and tailored folding by local heat-treatment. Mater. Des., 2016, 110: 157–168.
[5] Yuan X Y, Chen L Q, Zhao Y, et al. Influence of annealing temperature on mechanical properties and microstructures of a high manganese austenitic steel. J. Mater. Process. Technol., 2015, 217: 278–285.
[6] Wen Y H, Peng H B, Si H T, et al. A novel high manganese austenitic steel with higher work hardening capacity and much lower impact deformation than Hadfield manganese steel. Mater. Des., 2014, 55: 798–804.
[7] Jeong K, Jin J E, Jung Y S, et al. The effects of Si on the mechanical twinning and strain hardening of Fe-18Mn-0.6C twinning-induced plasticity steel. Acta Mater., 2013, 61: 3399–3410.
[8] Gwon H, Kim J K, Jian B, et al. Partially-recrystallized, Nb-alloyed TWIP steels with a superior strength-ductility balance. Mater. Sci. Eng. A, 2018, 711: 130–139.
[9] Mejía I, Salas-Reyes A E, Bedolla-Jacuinde A, et al. Effect of Nb and Mo on the hot ductility behavior of a high-manganese austenitic Fe-21Mn-1.3Al-1.5Si-0.5C TWIP steel. Mater. Sci. Eng. A, 2014, 616: 229–239.
[10] Scott C P, Remy B, Collet J L, et al. Precipitation strengthening in high manganese austenitic TWIP steels. Int. J. Mater. Res., 2011, 102(5): 538–549.
[11] Gutierrez-Urrutia I, Raabe D. Grain size effect on strain hardening in twinning-induced plasticity steels. Scripta Mater., 2012, 66(12): 992–996.
[12] Kang S, Jung J G, Kang M, et al. The effects of grain size on yielding, strain hardening, and mechanical twinning in Fe-18Mn-0.6C-1.5Al twinning-induced plasticity steel. Mater. Sci. Eng. A, 2016, 652: 212–220.
[13] Ma Y P, Li X L, Wang C H, et al. Microstructure and impact wear resistance of TiN reinforced high manganese steel matrix. J. Iron Steel Res. Int., 2012, 19: 60–65.
[14] Penna R V, Bartlett L N, O'Malley R. Influence of TiN additions on the microstructure of a lightweight Fe-Mn-Al steel. Inter. J. Metalcast., 2019, 14: 342–355.
[15] Fu J W, Nie Q Q, Qiu W X, et al. Crystallography and growth mechanism of TiN in Fe-17Cr stainless steel during solidification. J. Mater. Process. Tech., 2018, 253: 43–50.